Agricultural and Forest Meteorology 262 (2018) 120–134

Contents lists available at ScienceDirect

Agricultural and Forest Meteorology

journal homepage: www.elsevier.com/locate/agrformet

Temporal shifts in controls over methane emissions from a boreal bog

Mei Wang[a,b], Jianghua Wu[b,*], Peter M. Lafleur[c], Junwei Luan[d], Huai Chen[e], Xinbiao Zhu[f]

[a] School of Geographic Sciences, South China Normal University, Guangzhou, 510631, China
[b] Sustainable Resource Management, Memorial University of Newfoundland, Corner Brook, A2H 6P9, Canada
[c] School of the Environment, Trent University, Peterborough, ON, K9L 0G2, Canada
[d] International Center for Bamboo and Rattan, Beijing, 100102, China
[e] Key Laboratory of Mountain Ecological Restoration and Bio-resource Utilization & Ecological Restoration Biodiversity Conservation Key Laboratory of Sichuan Province, Chengdu Institute of Biology, Chinese Academy of Sciences, Chengdu 610041, China
[f] Atlantic Forestry Centre, Canadian Forest Service, Natural Resources Canada, Corner Brook, NL, A2H 5G4, Canada

ARTICLE INFO

Keywords:
Climate change
Non-growing season
Growing season
Seasonal pattern
Different time scales
Eddy covariance

ABSTRACT

We measured year-round landscape-scale methane (CH_4) flux in a boreal bog from May 2014 to April 2016 using the eddy covariance technique. The objectives of the study were to investigate the controls on CH_4 flux at different periods of the growing season and to quantify the annual CH_4 flux budget. The daily average growing season water table (WT) ranged from -0.33 to -0.08 m in 2014 and from -0.36 to -0.08 m in 2015. Strong seasonal variability in the daily average CH_4 fluxes was observed in both 2014 and 2015, ranging from near zero before May to a peak of above 20 nmol m^{-2} s^{-1} in the middle-late August in 2014 and in the early-middle September in 2015. Soil temperature at 50 cm and water table exerted interactive impact on the seasonal variation in the daily average growing season CH_4 flux in both years. Soil temperature at 1 cm was negatively related to CH_4 flux when water table dropped more than 0.25 m below the peat surface in 2015 growing season, suggesting that the seasonal variation in CH_4 flux was dominated by the variation due to CH_4 oxidation. During the non-growing season, the daily variation in CH_4 fluxes was mostly related to friction velocity in both years. In addition, daily average CH_4 flux was linearly related to net ecosystem exchange of CO_2 (NEE) when daily NEE was negative (i.e., days with CO_2 uptake larger than ecosystem respiration), but there was no correlation between them when NEE was positive (days with ecosystem respiration dominated over CO_2 uptake) during the growing season. We found that this boreal bog acted as a small CH_4 source of 3.7 $\pm$ 0.9 g CH_4 m^{-2} from May 2014 to April 2015 and 3.1 $\pm$ 0.9 g CH_4 m^{-2} from May 2015 to April 2016. These values were at the lower end of the range of CH_4 emission rates reported for boreal peatlands. Non-growing season CH_4 emissions accounted for 41% (the first study year) and 39% (the second study year) of the annual emissions, highlighting the importance of non-growing season CH_4 emissions in estimating the annual CH_4 budget and the feedback to climate.

1. Introduction

Methane (CH_4) is an important greenhouse gas, with the global warming potential about 25 times that of carbon dioxide (CO_2) on a 100-year time horizon (IPCC. Climate Change, 2014). The atmospheric CH_4 concentration has increased by 148%, from 715 ppb in pre-industrial times to 1774 ppb in 2005, and this trend is expected to continue in the future, thus it can exert a great impact on the future climate system (IPCC. Climate Change, 2014). The persistent increase in concentrations of atmospheric CH_4 has accounted for 20% of the total increase in radiative forcing over the past century (IPCC. Climate Change, 2014) and motivates efforts to understand the driving forces of different global CH_4 sinks and sources.

Northern peatlands are presently a sink of CO_2 but a source of CH_4 (Mikaloff Fletcher et al., 2004; Roulet, 2000). The ratio of CO_2 absorption to CH_4 emission largely determines the influence of peatlands on climate (Frolking et al., 2006). The effect of CH_4 emission variation was suggested to dominate the radiative forcing impact of peatlands on climate in the first few decades after their formation, after which the impact of the change in CO_2 sequestration slowly gained significance (Frolking et al., 2006; Frolking and Roulet, 2007). Currently, CH_4 emissions from peatlands contributes ~3–5% of the total global CH_4 emission (Mikaloff Fletcher et al., 2004; Prather et al., 2001). Estimated regional CH_4 emission rates of northern peatlands range from 32 to 112 Tg CH_4 yr^{-1} (1 Tg = 10^{12} g) (Bergamaschi et al., 2007, 2009; Petrescu et al., 2010; Zhuang et al., 2004).

* Correspondence author at: Sustainable Resource Management, Grenfell Campus, Memorial University of Newfoundland, Corner Brook, NL, A2H 5G4, Canada.
E-mail address: jwu@grenfell.mun.ca (J. Wu).

https://doi.org/10.1016/j.agrformet.2018.07.002
Received 23 March 2017; Received in revised form 29 June 2018; Accepted 2 July 2018
Available online 20 July 2018
0168-1923/

Much effort has been made in quantifying CH_4 emission rates and their contribution to the greenhouse gases balance of peatlands (Pypker et al., 2013) and in addressing the controls on the spatial and temporal variability in CH_4 flux, especially the relationship between CH_4 flux and environmental variables such as temperature, precipitation, water table, light and turbulence (Abdalla et al., 2016; Frenzel and Karofeld, 2000; Granberg et al., 1997; Günther et al., 2014; Lai et al., 2014; Liblik et al., 1997; Moore and Knowles, 1989; Treat et al., 2007; Turetsky et al., 2014). Yet, previous research has shown that the CH_4 emission rates can range over three orders of magnitude among northern peatland ecosystems (Koebsch et al., 2015; Turetsky et al., 2014; Vanselow-Algan et al., 2015; Zhuang et al., 2006) and that the variables most closely associated with CH_4 flux are not consistent among different peatland types (Abdalla et al., 2016; Turetsky et al., 2014), among microtopographies within the same peatland (Bubier et al., 1993; Nilsson et al., 2001; Skov, 2014) and at different timescales (Günther et al., 2014; Koebsch et al., 2015). Coupled with varying mechanisms of CH_4 production, transport and consumption, the wide fluctuations in reported CH_4 emission rates and changing driving forces pose a significant challenge in accurately estimating the CH_4 budget of peatlands at a global scale and for model development and testing (Bridgham et al., 2013).

In general, soil or air temperature and water table depth have been found to exert the greatest impact on the CH_4 emission dynamics at varying timescales (Frenzel and Karofeld, 2000; Granberg et al., 1997; Günther et al., 2014; Koebsch et al., 2015; Long et al., 2010; Mikkelä et al., 1995; Moore and Knowles, 1989; Pypker et al., 2013; Treat et al., 2007). Although in some casesthese environmental effects can be overshadowed by changes in the substrate availability for CH_4production(Koebsch et al., 2013; Pypker et al., 2013)and plant-driven gas transport (Chen et al., 2010; Kowalska et al., 2013). In the most extensive comparison of CH_4 fluxes from wetlands to date, Turetsky et al. (2014) found that peatland type was important in determining sensitivity of CH_4 flux to water table and temperature. Pristine bogs were more sensitive to soil temperature than other wetland types and this relationship can be tempered by antecedent water tables. The importance of the interaction between water table and temperature on CH_4 flux in bogs is well noted elsewhere (Granberg et al., 1997; Goodrich et al., 2015; MacDonald et al.,1998; Pypker et al., 2013; Turetsky et al., 2008), but such relationships are not universal or straightforward. As Brown et al. (2014) showed, the relationship between CH_4 flux and water table at the Mer Bleue bog was non-monotonic, where the largest fluxes were produced when water table was in a critical zone at depth below the peat surface and the confounding relationship between temperature and CH_4 flux increased the complexity of predictive models. Still others have found very simple relationships between temperature and CH_4 flux, with little to no influence from water table (Olson et al., 2013). Given these contrasting results, more observations are needed in these peatland ecosystems to further explore the range of responses to these environmental controls on CH_4 flux.

In this study, we report two years of field-scale CH_4 fluxes measured by eddy covariance at an undisturbed boreal bog in an attempt to investigate the seasonal and inter-annual variation of the CH_4 flux, to identify the controls on CH_4 flux at different timescales and quantify the annual CH_4 budget. We hypothesized that 1) there would be a strong seasonal and inter-annual variations in the CH_4 flux, 2) the controls over CH_4 fluxes would vary at these different timescales, and 3) this bog would act as an annual CH_4 source as suggested by previous chamber measurements at the bog (Luan and Wu, 2015).

2. Materials and methods

2.1. Study site

Our site, an undisturbed boreal bog, is located in the Robinsons pasture Western Newfoundland, Canada (48.260 N, 58.663 W). According to the data from the nearest weather station in Stephenville (48.541 N, 58.55 W)

(http://climate.weather.gc.ca/climate_normals/results_1981_2010_e.html?stnID=6740&autofwd=1), the average annual temperature of 1981–2010 is estimated at approximately 4.5 °C and the annual rainfall is ~955 mm. Details of site characteristics can be found in Luan and Wu (2014), and are only described briefly here. The bog, about 200 ha, consists of different landforms mainly including peatland pools, hollows and hummocks. The peatland pools varied significantly in size, ranging from 10 to 200 m^2, and were permanently inundated with the standing water depth of 40–60 cm. They cover only about 10% of the bog. The hollow and hummock landforms have a substrate mostly covered with bog moss species [*Warnstorf's peat moss (Sphagnum Warnstorfii) and Red peat moss(Sphagnum capillifolium)*]and partly with reindeer lichens *(Cladina* spp.*)*. Sedge [*Tufted bulrush (Trichophorum cespitosum)*]andherbs[*Deergrass (Muhlenbergia rigens,* cloudberry*(Rubus chamaemorus), Canadian dwarf cornel (Cornus Canadensis) and* club-mosses (*Lycopodiopsida)*]dominate the wetter hollow but ericaceous shrubs[huckleberry (*Gaylussacia* spp.*),*black crowberry (*Empetrum nigrum),* sheep laurel (*Kalmia angustifolia),* bog Labrador tea (*Rhododendron groenlandicum*)and bog Rosemary *(Andromeda polifolia*)]mainly occur on the drier hummock. The growing season water table level averaged 22 cm below the surface in the hollow and 32 cm below the surface in the hummock. Hollows and hummocks each account for about 45% of the bog area. The dry aboveground biomass, measured in 2013, was 197 ± 87 g m^{-2} in hummocks, similar to that of 191 ± 41 g m^{-2} in hollows. Dry root biomass was 745 ± 200 g m^{-2} in hummocks, significantly higher than that of 421 ± 141 g m^{-2} in hollows ($P < 0.05$) (Luan and Wu, 2015).

2.2. CH_4 flux and meteorological measurements

CH_4 flux measurements were made with an eddy covariance (EC) system (Fig.1). Wind vectors (u, v, w) and sonic temperature were measured with a three-dimensional (3-D) sonic anemometer (Gill WindMaster Pro, Gill Instruments) mounted at 3.44 m height above the mean surface of the bog. An open path infrared gas analyzer (LI-7700, Li-Cor Inc., Nebraska, USA) mounted at 3.34 m height, with the separation from sonic anemometer of 17 cm northward, -1 cm eastward and 10 cm vertically to measure CH_4 molar density. A fast response infra-red gas analyzer (IRGA: LI-7200 Enclosed CO_2/H_2O Analyzer, Li-Cor Inc., Nebraska, USA) was used to measure variations in CO_2 and H_2O molar densities. The LI-7200 analyzer was mounted at the height of 3.21 m with the separation between the sonic and IRGA being 3.5 cm northward, 3.5 cm eastward and 23 cm vertically. Air was pulled by a diaphragm pump through a 1 m long sample tube to the IRGA at a rate of 16.07 l min^{-1}. Instantaneous CO_2 and H_2O concentrations were measured inside the sampling cell, along with instantaneous air temperature and air pressure. The enclosed LI-7200 analyzer outputs not only instantaneous gas density for traditional flux calculations (Webb et al., 1980), but also instantaneous mixing ratio of CO_2 and H_2O, which use instantaneous water, temperature and pressure measurements inside the cell to correct for dilution, temperature and pressure. Two thermocouples were used to measure the instantaneous temperatures of air just before entering and exiting the sampling volume. A differential pressure sensor with a high speed and precision, together with a low speed, high precision absolute pressure sensor were used to measure instantaneous pressure in the middle of the cell. Data output from the EC system instruments were recorded at 10 Hz with a data logger (LI-7550, Li-Cor Inc., Nebraska, USA) and stored on a removable USB device.

Environmental variables were recorded by a series of meteorological instruments mounted on the EC system tower. Photosynthetically active photon flux density (PPFD) was measured by quantum sensor (LI-190SL-50, LI−COR Inc., Nebraska, USA). Air

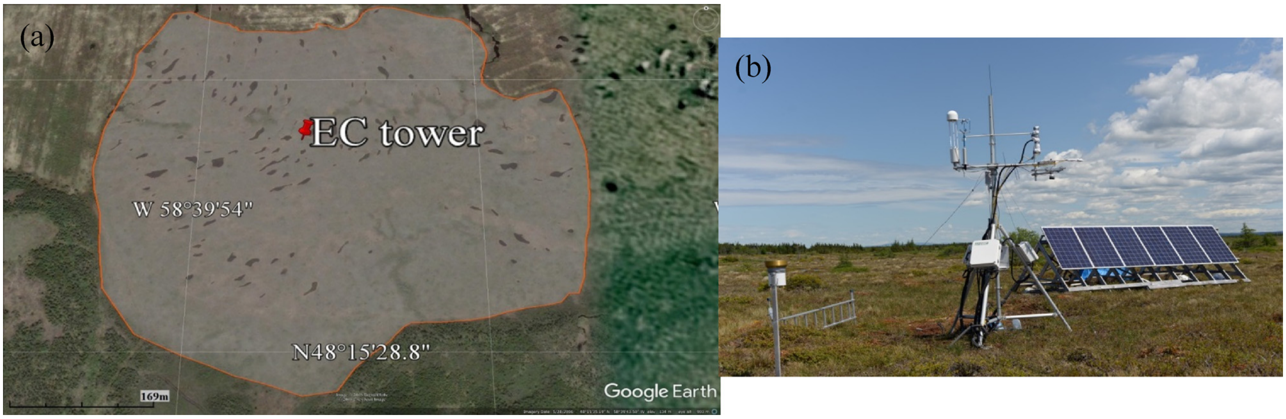

Fig. 1. Satellite image of the natural boreal bog at the Robinsons pasture, western Newfoundland, Canada (48.260 N, 58.663 W). The image was obtained from Google Earth with imagery collected on May 28, 2006. The outline of the site was indicated by the red solid line and the red pin represents the location of eddy covariance (EC) tower (a); (b) a photo of the setup of EC measurement system. (For interpretation of the references to colour in this figure legend, the reader is referred to the web version of this article).

temperature (Ta) and relative humidity (RH) was measured with a temperature / relative humidity probe (HMP155, Vaisala, Vantaa, Finland). A 4 − COmponent net radiometer (CNR4, Kipp & Zonen, Delft, The Netherlands) was amounted at a height of ∼3.5 m to monitor the incoming and reflected short-wave and long-wave radiation. A tipping-bucket rain gauge (TR-525USW, Texas Electronics, Texas, USA) was mounted on the ground to measure rainfall. Soil temperature was measured at depths of 1 cm, 5 cm, 10 cm, 30 cm and 50 cm below *Sphagnum* moss surface by thermistors (LI7900-180, Li-Cor Inc., Nebraska, USA) and soil moisture was measured as volumetric water content at 5 cm, 10 cm, 30 cm and 50 cm with a water content probe (Delta-TML2x, Delta-T Devices, U.K.). Water table depth (WTD), defined by using the surface of mosses as the zero datum, was monitored by a stainless steel pressure transducer sensor with SDI-12/RS232 connection (CS451, Campbell Scientific, Utah, USA). Rainfall was recorded as 30-min totals, and all other environmental variables were scanned at 5-s intervals and recorded as half-hourly means on a data logger (CR3000-XT, Campbell Scientific, Utah, USA).

2.3. Data processing

2.3.1. Data quality control, and gap filling and partitioning

We used EddyPro 5.2.1 software (Li-Cor Inc., Nebraska, USA) to process the 10 Hz raw data from the EC system and output corrected fluxes of CH_4 and CO_2 over a 30-min interval. In this study default settings for analytical corrections were applied to adjust for air density fluctuations by Webb-Pearman-Leuning for CH_4 flux (Webb et al., 1980), corrections for frequency response (Moncrieff et al., 2004, 1997), double axis rotation for sonic anemometer tilt correction (Wilczak et al., 2001), statistical control tests for fluxes (Vickers and Mahrt, 1997), quality control tests for fluxes (Mauder and Foken, 2011), flux footprint estimation (Kljun et al., 2004), lag minimization using maximum covariance with default lag of 0, and calculation of friction velocity (u*) using both along and cross wind shear. The analytical corrections mentioned above were only applied to methane flux data. The frequency corrections, which included a component for path averaging, can be large, averaging 11.6% in 2014–15 growing season, 13.5% in 2014–15 non-growing season, 12.2% in 2015–16 growing season and 8.9% in 2015–16 non-growing season.The data from the enclosed-path CO_2 analyzer was analyzed with a data-driven method and the detailed method for the data processing for the enclosed-path CO_2 analyzer was presented in Wang et al. (2018).The data quality of the corrected half-hourly fluxes were indicated by the values of diagnostic flags, with 2 representing data of bad quality (Mauder and Foken, 2011) and these data were discarded.The half-hourly flux data during periods of rainfall were also discarded. The half-hourly CH_4flux data with signal strength value less than 10 were also discarded. The final flux data was corrected by adding the storage flux below the height of the CO_2 and CH_4 analyzer, computed from half-hourly mean concentration changes at the sensor level.

Fetch in the bog varied from about 270 m to 400 m in different directions. We used this information to filter the fluxes as follows. Data with the 70% footprint larger than 380 m with wind direction of 0–180° and larger than 300 m in the sector 180–360° were rejected in order to guarantee the fluxes source are mostly from within the bog boundary. In addition, we did not find threshold value of u* above or below which CH_4 flux increased or decreased significantly, so no u* filtering was applied. Approximately 58% (2014) and 45% (2015) of the growing season CH_4 flux data and 53% of the non-growing season flux data in both study years were rejected due to bad data quality and instrument failure.

Gaps in the CH_4 flux data were fill using an artificial neural network (ANN). This method is one of a suite of tools being used for gap-filling in flux studies (Moffat et al., 2007; Papale et al., 2006) and has been shown recently to be highly successful for gap-filling CH_4 fluxes (Dengel et al., 2013). The ANN was performed using the Matlab numerical software. Data were divided into clusters of daytime and nighttime according to the PPFD threshold of 20 μmol m^{-2} s^{-1}. 70% of available date in each cluster was used to train the network, an additional 15% for testing the network and finally, 15% for validating the ANN. Before training, all data were normalized as 0–1 as in (Aubinet et al., 2012; Dengel et al., 2013; Moffat et al., 2010; Nguyen and Chan, 2004). The architecture of each neural network was initialized 10 times with random starting weights, and the initialization resulting in the lowest mean sampling error was used (Järvi et al., 2012). The simplest architecture, whereby additional increase in complexity resulted in less than 5% decreasein mean square error, was selected and the prediction was saved. Therefore, we set the number of neurons in the fitting network's hidden layer as 10. This procedure was replicated 20 times and the median predictions were used to fill missing half hour fluxes. The neural network includes an input layer, a hidden layer and an output layer (Elizondo and Góngora, 2005; Jain et al., 1996) and this two-layer feed-forward network with sigmoid hidden neurons and linear output neurons can fit multi-dimensional mapping problems arbitrarily well. The ANN was trained with the Levenberg-Marquard backpropagation algorithm in MatLab (trainlm), as used in previous studies (Dengel et al., 2013; Riedmiller, 1994). We chose input variables including air temperature, surface soil temperature, subsurface soil temperature, solar radiation, vapor pressure deficit (VPD), u* and WTD according to a previous study (Dengel et al., 2013). However, during some periods in

wintertime, VPD and u* data were also missing, so we only used the remaining variables mentioned above to fill the data gaps at these times. Gap-filled flux data were only used for CH_4 budgeting in this analysis.

We partitioned CH_4 fluxes into four periods as in Song et al. (2015): the growing season and three non-growing seasons including soil thawing, soil freezing and winter. Growing season began and ended at the first seven consecutive days with daily air temperature above 5 °C and below 5 °C, respectively. We further subdivided the growing season into three periods of early growing season (May and June), peak growing season (July and August) and late growing season (September, October and November). Soil freezing, ranging from the end of the growing season to the first two consecutive days with average daily soil temperature below 0 °C at 5 cm depth. Winter started at the end of the soil freezing period and ended when snow melted out (after seven consecutive days with average air temperature above 0 °C). The soil thawing period was between winter and the growing season. The purpose of partitioning CH_4 into different periods was to estimate the contribution of cumulative CH_4 flux in each period to the annual flux budget, as well as to examine the variations in the controlling factors of CH_4 flux in different growing season periods and the non-growing season. We did not find any significant CH_4 burst during the soil freezing and thawing periods and the data availability of these two periods were limited. Therefore, we lumped all non-growing season period together to identify the environmental controls on the CH_4 flux.

2.4. Flux uncertainty estimation

Although there are many sources of uncertainty in flux estimation measured by eddy covariance, here we focused on flux random uncertainty due to sampling errors. The other uncertainty sources [e.g., errors due to the buoyancy effects of heat and water vapor, errors due to limited response time of the sensors, errors due to separation of the sensors, errors due to random noise in the system, errors due to inadequate or excessive height of the sampler over the surface, errors due to inadequate fetch, errors due to flow distortion caused by aerosol particles, and etc.] can be reduced due to either properly field experiment design (Businger, 1986)or flux data correction as mentioned above. Some of the uncertainties could be important such as the uncertainty caused by the design of the open-path LI-7700 sensor. We made the frequency response corrections, part of which included a component for path averaging using the standard data processing procedures as presented in Moncrieff et al. (1997, 2004). Therefore, our final output CH_4 flux included the impact of path averaging of the LI-7700 sensor. Yet, sampling error remains as one of the largest sources of uncertainty. Flux random uncertainty (σ_1) in EddyPro was calculated following Finkelstein and Sims (2000). This method requires the preliminary estimation of the Integral Turbulence Time-Scales, which can be defined as the integral of the cross-correlation function between vertical wind component and any scalar of interest (e.g. temperature, gas concentration, etc.), details can be found in (Finkelstein and Sims, 2001). We also estimated the flux uncertainty due to gap-filling (σ_2) based on the following procedures. Firstly, we developed, trained and validated ANN model using the available measured data in each study period (i.e., growing season, soil freezing period, soil thawing period and wintertime). Secondly, we ran the ANN model and produced a continuous series of data for the whole two-year study period. Finally, we randomly chose 30% of the available measured datathat were not used to train the ANN model and comparedthem with their counterpart predictedCH_4 flux values from ANN model in each study period (Moffat et al., 2007). $\sigma_2 = 1 / N \sum (Pi - Oi)$. N is the number of measured and predicted CH_4 flux pairs in a certain period and P_i and O_i are the individual predicted CH_4 flux data and the observed value, respectively. The total uncertainty was calculated following the equation: $\sigma = [\sigma_1^2 + \sigma_2^2]^{1/2}$.

2.5. Statistical analysis

We used surface plots to visualize the interactions between WT, T_{50} and CH_4 flux during different growing season periods. In order to better understand the role of WT and soil temperature on CH_4 flux, we used nonlinear regression models to explore the relationship between CH_4 flux and water table under different soil temperature ranges [$T_{50} < 5$ °C, 5–7 °C, 7–9 °C, 9–11 °C, 11–13 °C and > 13 °C]. When studying the exponential relationship between soil temperature and CH_4 flux, we classified data into several groups based on different WT conditions (WT: −0.1 ~ −0.15 m, −0.15 ~ −0.20 m, −0.20 ~ −0.25 m, −0.25 ~ −0.30 m, −0.30 ~ −0.35 m). There were many rapid WT rises and drops following large rainfall (> 2 mm), so we studied the effect of large rainfall on CH_4 flux by comparing the daily average flux one day before rainfall day, rainfall day and one day after rainfall day. One-sided paired t-tests were used to make the statistical comparisons of CH_4 flux among periods (SAS 9.1Institute, Cary, NC, USA).

3. Results

3.1. Seasonal variation in environmental variables

Air temperature during the study tended to be close to long-term normal (within ± 1 standard deviation of long-term averages) with the exceptions of higher than normal temperature in July 2014 and August 2015 and lower than the long-term averages in March and April of 2015 (Fig.2a). Daily air temperatures ranged from −16.6 °C to 23.6 °C in 2014–15 peaking in the middle of July in 2014 and from −11.2 °C to 21.6 °C in 2015–16 with the maximum values in middle-late August and the lowest values in the end of February of both years (Fig. 3a). Annual average air temperature was 4.4 °C in 2014–15 and 4.7 °C in 2015–16 (Table 1). The seasonal pattern of soil temperature was similar to that of air temperature, except for a leveling-off of minimum temperatures between January and April, while the peatland was snow covered (Fig. 3b). The coldest subsurface soil temperature (at 50 cm, T_{50}) occurred at the end of April when snow melted out and the warmest occurred near early-middle August in 2014 and in early September in 2015, almost 2 weeks later than of the maximum air temperature (Fig. 3b).

The daily average growing season WT in a hollow ranged from −0.33 to −0.08 m in 2014 and from −0.36 to −0.08 m in 2015, with several episodes of rapid rises and drops in both years following summer rainfall events (Fig. 3d,e). The drier than normal conditions of September 2015 resulted in decline of ~8 cm in the monthly average WT compared with that of 2014 (Fig. 2b, Fig. 3d, Table S1).

The growing season WT averaged −0.21 m in 2014 and −0.23 m in 2015 (Table 1). Soil moisture at 30 cm followed a similar pattern as WT and ranged from ~0.76 to 0.88 $m^3 m^{-3}$ over the study period (Fig. 3c,d). The growing season cumulative rainfall was 513 mm in 2014 and 585 mm in 2015 and the yearly cumulative rainfall was 942 mm in 2014–15 and 890 mm in 2015–16 (Table 1). These werecomparable to the long-term average (955 ± 133 mm).

3.2. Seasonal variation in CH_4 flux

Daily average CH_4 flux showed strong seasonal variability in both 2014 and 2015 (Fig. 4). The CH_4 emission ranged from near zero in the early May to a peak between 20 to 30 nmol $m^{-2} s^{-1}$ that occurred in the mid-late August in 2014 and in early-mid September in 2015. Fluxes then decreased to near zero by the end of the growing season. The growing season CH_4 flux peak occurred about ten days later than the maximum subsurface soil temperature at 50 cm (Figs. 3b & 4). During the non-growing season periods, CH_4 fluxes were quite noisy, ranging from approximately −10–20 nmol $m^{-2} s^{-1}$. There were no observed pulses in daily average CH_4 flux during soil freezing or thawing periods.

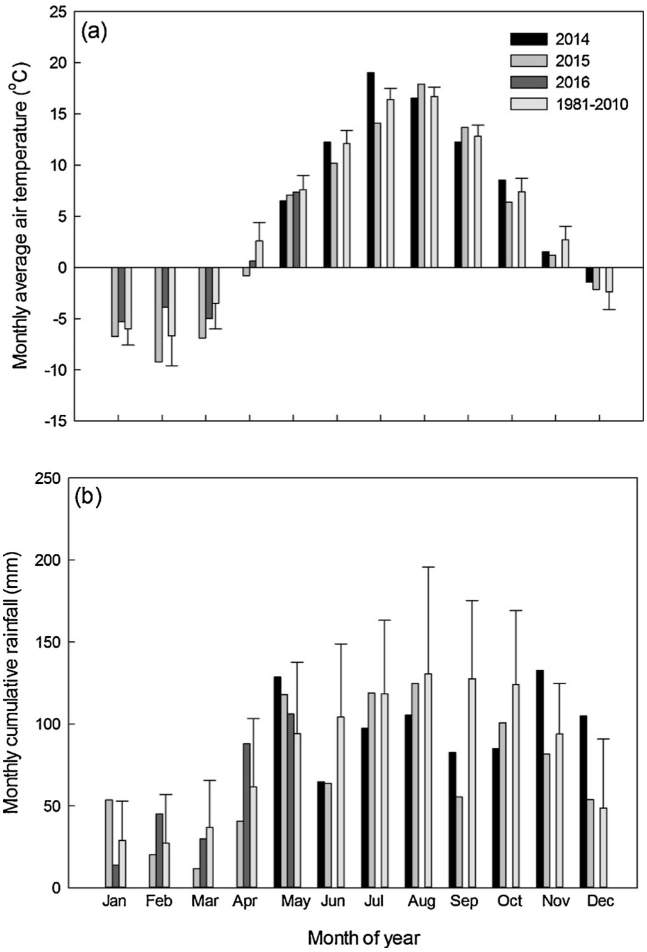

Fig. 2. Comparison of monthly average temperature and cumulative monthly rainfall measured at the pasture during measurement periods from April 2014 to May 2016 with the long-term (30 years average ± SD) measurement of the nearby climate station at Stephenville, Newfoundland and Labrador during.1981–2010.

3.3. The biotic and abiotic controls over daily CH_4 flux

Our results indicated that WT and T_{50} affected the CH_4 flux interactively, but their interactive effects varied among different growing season periods (Fig.5). During the early growing season, CH_4 flux increased with the increase in T_{50}under different WT conditions. During the middle growing season, CH_4 flux steadily increased with T_{50}, with the highest emission rates occurring when both WT and T_{50}were high. During the late growing season, CH_4 flux generally increased with an increase in WT (when WT approaching the peat surface) and T_{50}, with high emissions occurring when either of the two variableswas high.

We studied the impact of soil temperature on CH_4 flux by classifying data into several groups according to different WT ranges to eliminate the confounding effect of WT (Figs. 6 and 7). Our results showed that T_{50} had a strong positive effect on CH_4 flux under varying WT conditions in both growing seasons (Fig. 6). We found that T_1 had a negative impact on CH_4 flux in 2015 when water table dropped 0.25–0.30 m below the peat surface (Fig. 7h,j), while CH_4 flux was positively related to the variation in T_1 when WT was above 0.30 m below peat surface in 2014 (Fig. 7a,c,e,g) and between −0.20 m and −0.15 m in 2015 (Fig. 7d).

We studied the impact of WT on growing season CH_4 flux under different T_{50} ranges and found a positive correlation between CH_4 flux and WT when T_{50} was above 7 °C in 2014 and above 9 °C in 2015 (Fig. 8). A negative relationship between WT and CH4 flux was found when T_{50} was below 5 °C in 2015 (Fig. 8b).

In addition, we studied the effect of large rainfall events (> 2 mm) during the middle growing season on CH_4 flux by comparing the fluxes among one day pre-rainfall, rainfall day and one day after rainfall (Fig. 9a,b). We found that on average CH_4 flux was the highest for the post-rainfall day for both years and the overall CH_4 flux was significantly higher than its counterparts for pre-rainfall day and rainfall day (Fig. 9c,d).

A previous study based on chamber measurements at this site suggested that substrate availability also plays an important role in regulating growing season CH_4 flux (Luan and Wu, 2015). Therefore, we investigated the relationship between net ecosystem exchange (NEE, an indicator of substrate availability) and CH_4 flux. We found that the daily average growing season CH_4 flux increased with enhanced daily average CO_2 uptake rate when NEE was negative. However, there was no correlation between CH_4 flux and NEE when the daily average NEE was positive (Fig. 10).

3.4. Annual CH_4 flux budget and uncertainty estimation

The accumulated annual CH_4 flux, estimated from observations and ANN gap filling, was ~3.7 ± 0.9 g $CH_4\,m^{-2}$ in 2014-15 and 3.1 ± 0.9 g CH_4 m^{-2} in 2015-16 according to ANN gap filling (Table 2). Contributions of the growing season and non-growing season were similar among the two years.The flux uncertainty was caused more by the random error in 2014–15 but by the gap-filling in 2015-16 of about 18% and 25% of the cumulative flux, respectively (Table 2). In our estimation of the annual methane budget, we did not use a u* threshold to exclude any flux data. The CH_4 budget without the u* threshold was 3.7 g $CH_4\,m^{-2}$ in 2014-15 and 3.1 g $CH_4\,m^{-2}$ in 2015-16, which was not significantly different from the budget of 3.6 g $CH_4\,m^{-2}$ in 2014–15 and 3.1 g $CH_4\,m^{-2}$ in 2015–16 where we used 0.1 m s^{-1} as the u* threshold value. Therefore, our annual CH_4 budget does not depend on a friction velocity threshold. Though the growing season CH_4 emissions contributed the greatest amount to the annual total emissions in both years, the non-growing season emissions, which accounted for 41% (2014-15) and 39% (2015-16) of the total, were also important components of the annual budget (Table 2).

4. Discussion

4.1. Controls on the seasonal variation in daily CH_4 flux

We found that soil temperature and water table affected the CH_4 flux interactively at this boreal bog and their interactive effects varied among different growing season periods. During the early growing season, the CH_4 flux was more controlled by T_{50} than WT, similar to previous findings that CH_4 flux was more dependent on soil temperature than water table under cold conditions(Turetsky et al., 2014; Lai et al., 2014). Indeed, we found no significant positive relationship or even a negative correlation of WT and CH_4 flux when T_{50} was below 7 °C in 2014 and 9 °C in 2015. This is probably due to the overriding effect of low soil temperature, which limited CH_4 production due to low activity of methanogenic bacteria and reduced substrate availability (Turetsky et al., 2014). During the middle growing season, CH_4 flux was positively related to both WT and T_{50}, with the highest CH_4 flux occurring when both variables were high, as suggested previously (Turetsky et al., 2014). During the late growing season, high CH_4 high emissions occurred when either T_{50}or WT was high, suggesting shifting dominant controls on CH_4 flux.

In order to eliminate the confounding effect of WT on CH_4 flux, data were classified into different groups based on WT ranges. We found that $T_{50}$was strongly linked to variation in growing season CH_4 flux under different WT conditions in both 2014 and 2015, which is consistent with previous studies showing that soil temperature is fundamental control on CH_4flux in undisturbed peatlands (Turetsky et al., 2014). The

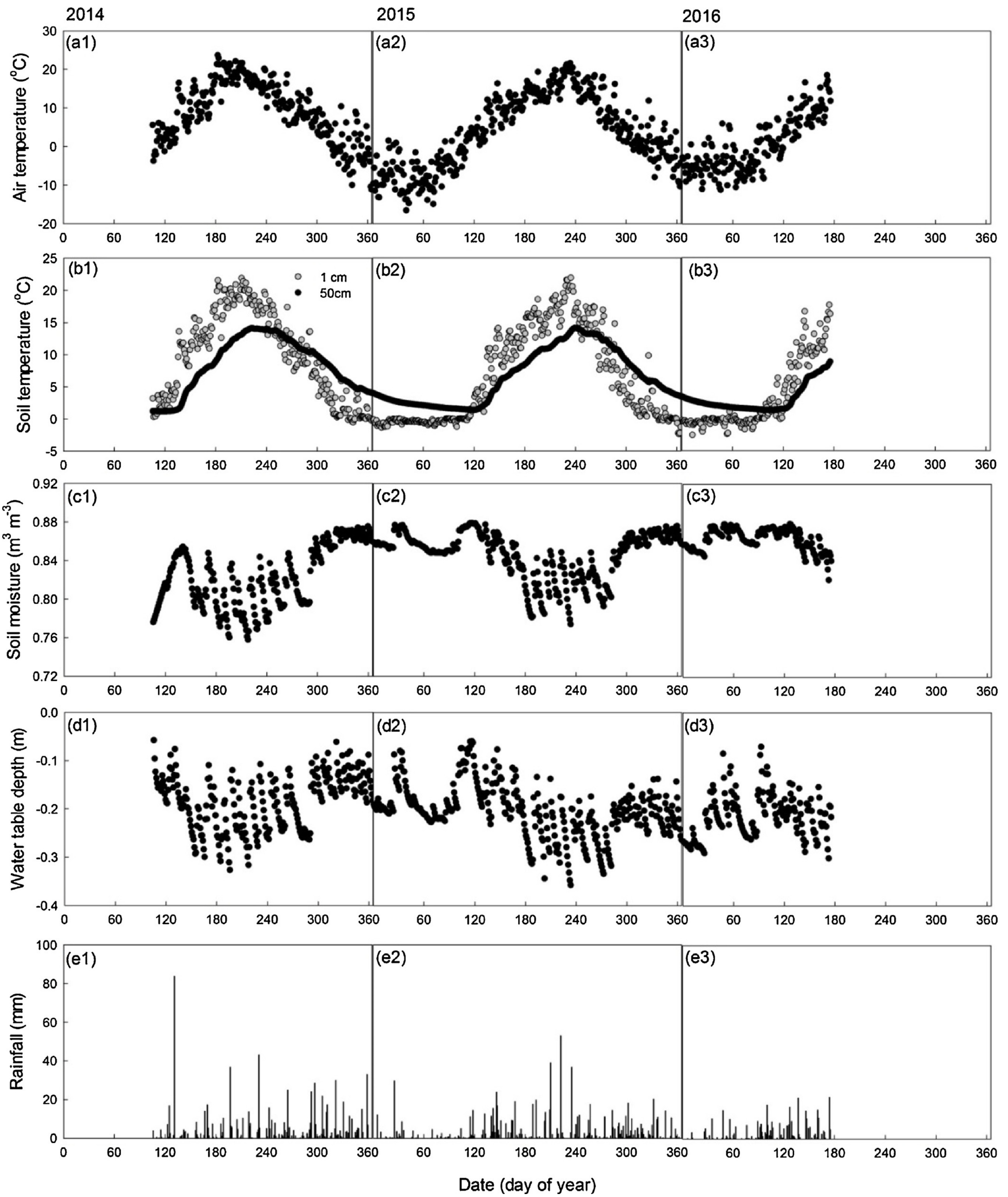

Fig. 3. The daily average air temperature (a1-a3), soil temperature at 1 cm and 50 cm (b1-b3), volumetric soil water content at depth of 30 cm (c1-c3), water table depth (d1-d3) and cumulative rainfall (e1-e3) during the measurement period.

CH_4 flux comes from the difference between methane production and methane oxidation, two counteracting processes. Both processes are temperature sensitive, which makes the control of temperature on CH_4 flux being complex and depending on the water table position (Goodrich et al., 2015). The strong subsurface soil temperature control arises because of its direct impact on the processes of CH_4 production, which are regulated by the activity of methanogenic bacteria (Metje and Frenzel, 2007). The positive relationship between CH_4 production and temperature has been well established in peatlands (Svensson, 1984; Williams and Crawford, 1984). In addition, we found the

Table 1
Average daily air temperature, soil temperature at depth of 1 cm, 10 cm and 50 cm, photosynthetic photon flux density (PPFD), cumulative rainfall, and water table depth for four different periods in the two study years.

Period		Date	Air temperature	Soil temperature (°C)			PPFD	Rainfall	WTD
			(°C)	1 cm	10 cm	50 cm	(mol m^{-2} d^{-1})	(mm)	(m)
Growing season	Early	2014.5.15-6.30	11.4	12.4	9.4	5.9	38.2	81	−0.21
	Middle	2014.7.1-8.31	18.0	18.5	16.9	12.7	35.5	203	−0.23
	Late	2014.9.1-11.8	9.8	10.4	11.1	11.4	18.6	229	−0.19
	Overall	2014.5.15-11.8	13.1	13.7	12.7	10.4	29.7	513	−0.21
	Early	2015.5.16-6.30	10.2	10.9	9.3	6.2	33.6	161	−0.18
	Middle	2015.7.1-8.31	16.1	17.0	15.3	11.5	32.1	244	−0.25
	Late	2015.9.1-11.15	8.5	9.3	10.4	11.0	14.1	181	−0.24
	Overall	2015.5.16-11.15	11.5	12.3	11.8	10.0	25.1	585	−0.23
Soil freezing		2014.11.9-2015.1.9	−1.9	1.0	2.7	5.4	5.0	191	−0.15
		2015.11.16-12.30	−1.2	0.7	2.4	4.9	4.9	92	−0.21
Winter		2015.1.10-2015.4.30	−5.6	−0.4	0.1	2.1	19.7	126	−0.17
		2015.12.31-2016.4.30	−3.4	−0.1	0.0	1.9	15.5	174	−0.22
Soil thawing		2014.5.1-5.14	2.6	3.7	0.1	1.2	36.4	112	−0.14
		2015.5.1-5.15	3.6	3.5	0.1	1.7	40.0	38	−0.16
Annual		2014.5-2015.4	4.4	6.9	6.7	6.7	22.7	942	−0.18
		2015.5-2016.4	4.7	6.4	6.2	6.3	20.0	890	−0.22

seasonal variation in CH_4 flux was negatively related to T_1 when WT dropped more than 0.25 m below peat surface in 2015 suggesting that CH_4 oxidation plays a role in regulating CH_4 fluxes under low WT conditions. We did not find this same relationship in the 2014 growing season, probably due to the over-riding positive impact of T_{50} on CH_4 flux since significant correlation between T_1 and T_{50}were found under different WT conditions (Fig. S2). It may also reflect the seasonality in plant production that was controlled by PAR and air temperature, which hada very similar seasonal pattern of T_1 (Fig. 3).

WT was found to be asignificant factor in regulating CH_4 flux when T_{50} was above 7 °C in 2014 and 9 °C in 2015, as has been shown previously (Turetsky et al., 2014).In addition, we found that the CH_4 flux was significantly increased after rainfall events. This is consistent with previous findings that drying and rewetting of peats stimulated CH_4 production (Dinsmore et al., 2009; Kim et al., 1999; Turetsky et al., 2014). Our results suggested that rainfall event could, to some extent, regulate the processes of C cycling in boreal peatlands. Nijp et al. (2015) also found that rainfall events could modulate the C cycling in boreal mires although their analysis focused on the CO_2 cycling. The exact mechanism(s) underlying the influence of rapid changes in WT on CH4 flux are still not completely understood, however it has been suggest that rapid WT change can significantly increase the CH_4 flux by either pushing the stored CH_4 out of the soil or by increasing the CH_4 production and reducing CH_4 oxidation (Turetsky et al., 2014). In addition, others have suggested that drying and subsequentrewetting of peat can lead to pulses of nutrients andwater-soluble products of decomposition, which maystimulate CH_4 production (Blodau et al., 2004; Kane et al., 2010). Overall, our findings imply that a wet climate in warm growing season periods will promote the CH_4 flux at this boreal bog.

Substrate availability has been recognized as important control over CH_4 fluxes in this bog (Luan and Wu, 2015) and in northern peatlands elsewhere (Alm et al., 1997; Bellisario et al., 1999; Christensen et al., 2003; Pypker et al., 2013; Waddington and Roulet, 1996; Whiting and Chanton, 1993). Bergman et al. (2000) found that substrate availability showed different impacts on the seasonal variation in CH_4 production for peats from different micro-topographies based on incubation experiments. We also found that varying functions of NEE on CH_4 flux under different daily CO_2 fixation capacity, where the daily CH_4 flux was linearly related with daily NEE when it was negative (indicating CO_2 uptake was large and dominated over ecosystem respiration) but when daily NEE was positive (ecosystem respiration dominated and production was small) no correlation between NEE and CH_4 flux existed (Fig. 10). Pypker et al. (2013) found similar results for a sub-boreal in northern Michigan. During the growing season, the increase in plant productivity inputs high quality organic matter into peat soils (Luan and Wu, 2015), thereby facilitating the anaerobic CH_4 production and hence CH_4 emission. We found the highest CH_4 flux lagged the maximum NEE by 30–40 days (not shown). Similarly, Lai et al. (2014) observed that the daily average CH_4 flux lagged 18–26 days behind

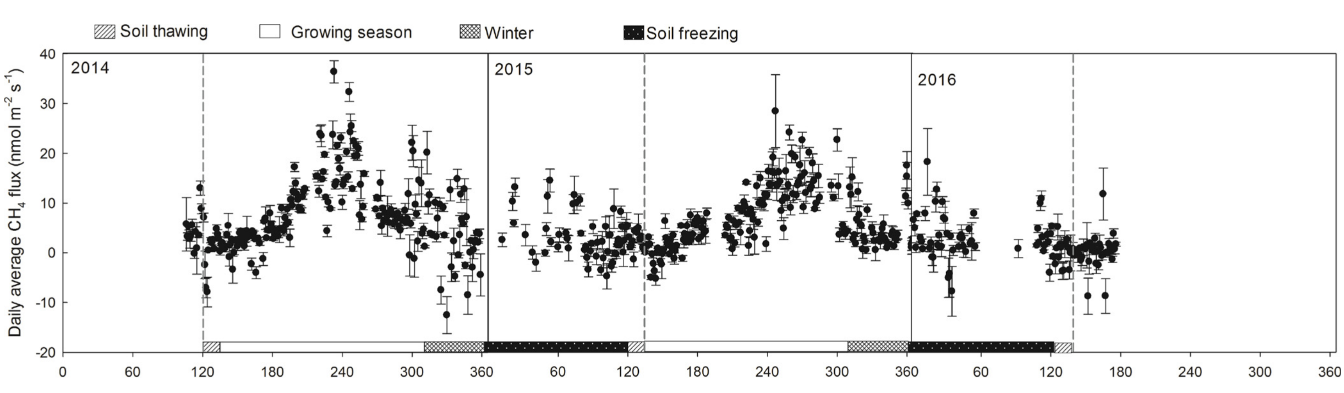

Fig. 4. The daily average CH_4 flux for different seasonal periods over the two measured years. Whiskers indicate standard error of the average. Growing season began and ended at the first seven consecutive days with daily air temperature above 5 °C and below 5 °C, respectively. Soil freezing, ranging from the end of the growing season to the first two consecutive days with average daily soil temperature below 0 °C at 5 cm depth. Winter started at the end of the soil freezing period and ended when snow melted out (after seven consecutive days with average air temperature above 0 °C). The soil thawing period was between winter and the growing season.

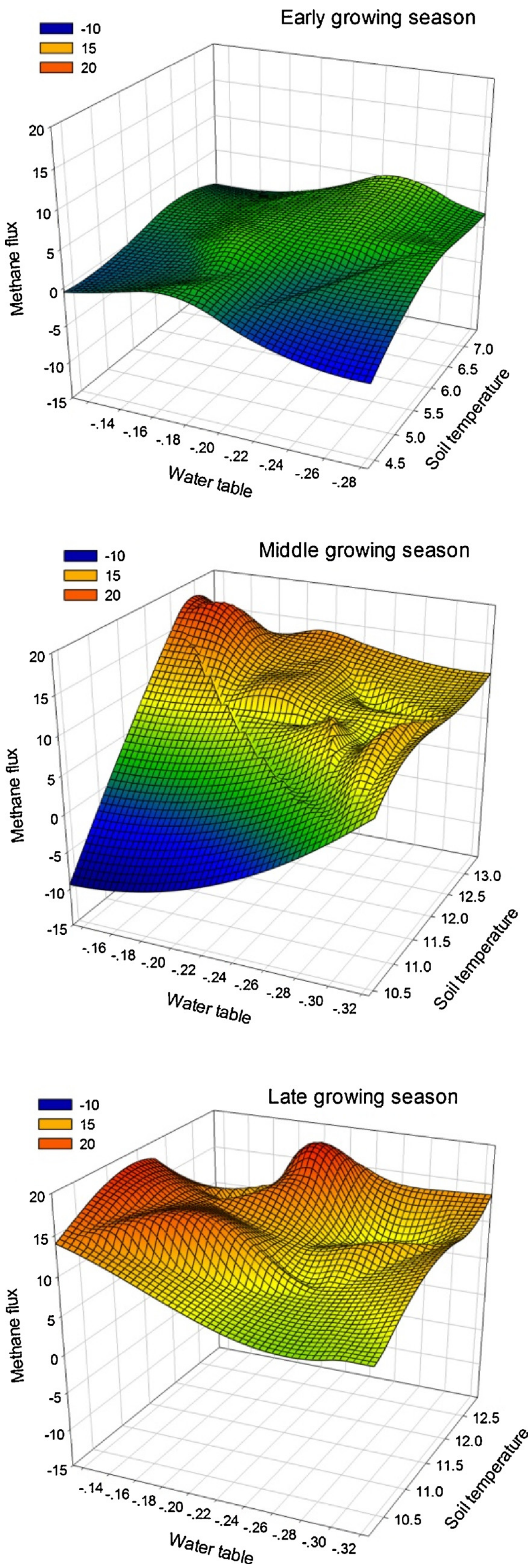

Fig. 5. Interactions between soil temperature at 50 cm and water table govern CH_4 flux. Surface plots of relationships between daily average CH_4 flux (nmol m^{-2} s^{-1}), soil temperature at 50 cm (°C), and water table position (m) for the early (a), middle (b) and late (c) growing season.

gross ecosystem production at Mer Bleue bog in Canada. These results further suggest that the CH_4 production potential may have been regulated by substrate availability from fresh OM input for this bog, as suggested by others (Liu et al., 2014). Overall, our results indicate that the growing season CH_4 fluxes were controlled by both abiotic factors (soil temperature and WT) and biotic factors (NEE).

During the non-growing season, the daily average CH_4 flux was weakly correlated only to u* and no other environmental variables (Fig.11). The relationship between u* and CH_4 flux has been reported in several previous studies of tundra ecosystems and lakes (Sachs et al., 2008; Wille et al., 2008), where increased turbulence leads to a transient flushing of CH_4 that was stored in near surface layers during calm periods in wintertime, leading temporarily to high CH_4 fluxes.

4.2. Comparison of the annual CH_4 fluxes between this bog and peatlands elsewhere

On the annual time scale, this boreal bog acted as a small source of CH_4, with emissions of 3.7 ± 0.9 g CH_4 m^{-2} yr^{-1} in 2014–15 and 3.1 ± 0.9 g CH_4 m^{-2} yr^{-1} in 2015–16 (Table 2). These values are within the lower range of the reported CH_4 rates in undisturbed peatlands elsewhere (Bridgham et al., 2013; Fortuniak et al., 2017; Hommeltenberg et al., 2014; Lai et al., 2014; Nilsson et al., 2001, 2008; Turetsky et al., 2014). In addition, growing season accumulated CH_4 fluxes of 2.2 ± 0.7 g CH_4 m^{-2} in 2014 and 1.9 ± 0.8 g CH_4 m^{-2} in 2015 were similar to the previous estimate for this bog of 1.8 g CH_4 m^{-2} in 2013 based on chamber measurements (Luan and Wu, 2015).

The non-growing season cumulative CH_4 emissions of 1.5 ± 0.5 g CH_4 m^{-2} in 2014–15 and 1.2 ± 0.4 g CH_4 m^{-2} in 2015–16 accounted for 41% and 39% of the total annual emissions, similar to that of 43–46% observed at an alpine wetland (Song et al., 2015) and 35% in a subarctic peatland (Jackowicz-Korczyński et al., 2010). Clearly, non-growing season emissions cannot be ignored and highlights the need for year-round CH_4 measurements when quantifying the annual CH_4budget. Although fluxes during the non-growing season are generally quite small, less than 1/2 that of average growing season emission rates at this bog, as well as in other peatlands (Jackowicz-Korczyński et al., 2010; Song et al., 2015), the long duration of winter in high latitude regions (~six months) leads to substantial accumulated losses.

In some studies high emission rates have been observed during soil freezing and thawing periods (Jackowicz-Korczyński et al., 2010). We did not find any evidence of spring-thaw or fall freezing induced CH_4 emission pulses. Nevertheless, our data indicate the importance of non-growing CH_4 flux in the annual CH_4 emission. Moreover, the data quality of non-growing season CH_4 fluxmeasured by the open-path LI-7700, due to the frequent snowing and other unexpected weather condition, was found to be much lower than the growing season CH_4 flux data. Therefore, there is a critical need for long-term non-growing CH_4 flux measurement in order to better elucidate the controls on the non-growing season CH_4 emission in boreal peatlands and their contribution to the overall annual budget.

5. Conclusion

We assessed the magnitude, patterns and environmental drivers of CH_4 fluxes in a boreal bog based on two years of ecosystem-scale measurements. Our study suggested that soil temperature and water table affected the ecosystem CH_4 exchange interactively, but the dominance of each variable differed among different growing season periods. Moreover, we hypothesize that temperature-related CH_4 oxidation played an important role in regulating CH_4 flux when water table dropped below −0.25 m. In addition, given that enhanced CH_4 flux was observed during large rain events in the growing season, it is particularly important to examine how future changes in the magnitude

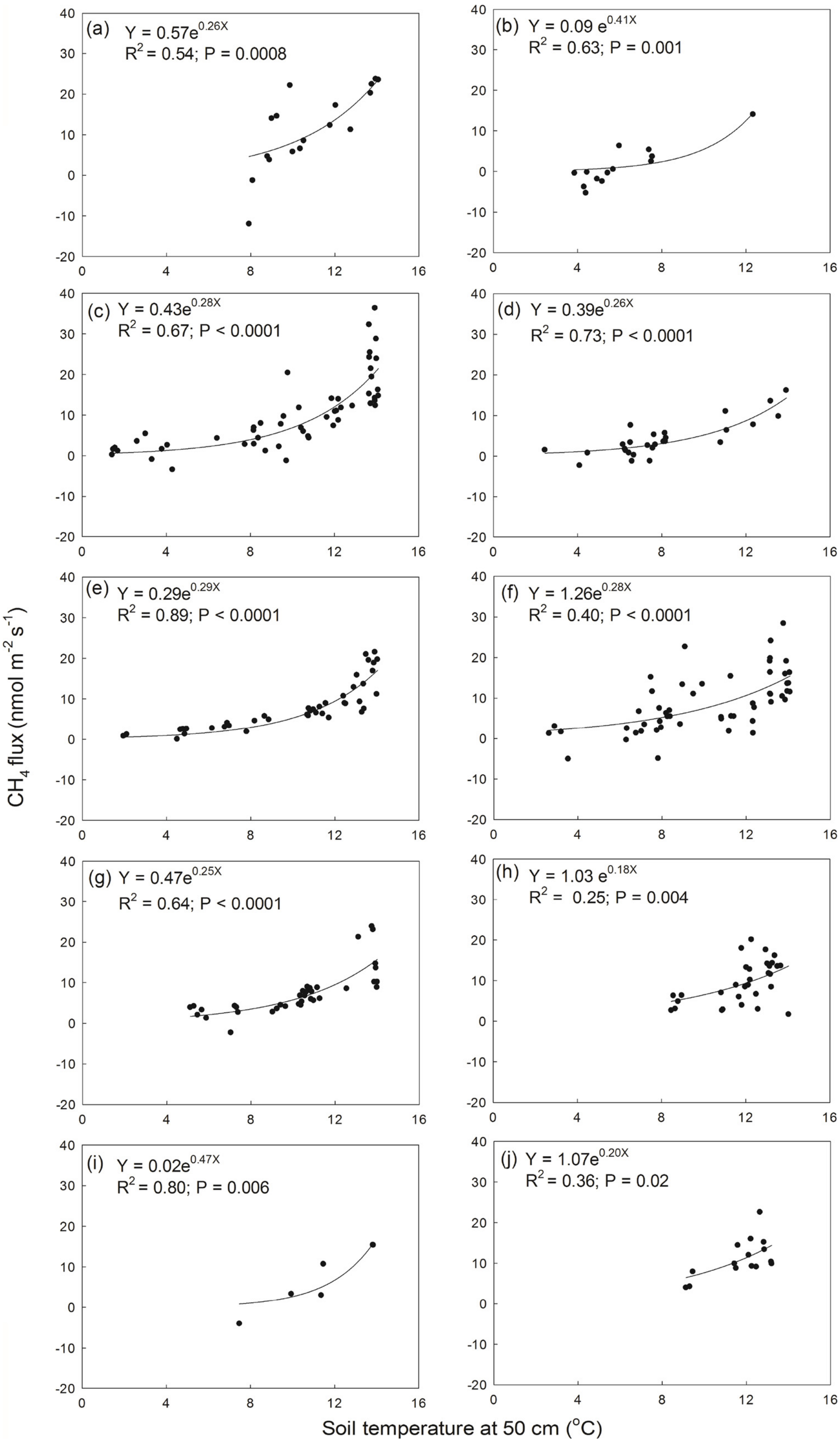

Fig. 6. The relationship between soil temperature at 50 cm and growing season CH_4 flux under different water table (WT) conditions. The left panel is for 2014 and the right one is for 2015. The panels from the top to the bottom were for WT range of -0.1 to -0.15 m (a, b), -0.15 ~ -0.2 m (c, d), -0.2 ~ -0.25 m (e, f), -0.25 ~ -0.30 m (g, h) and -0.30 to -0.35 m (i,*j*), respectively.

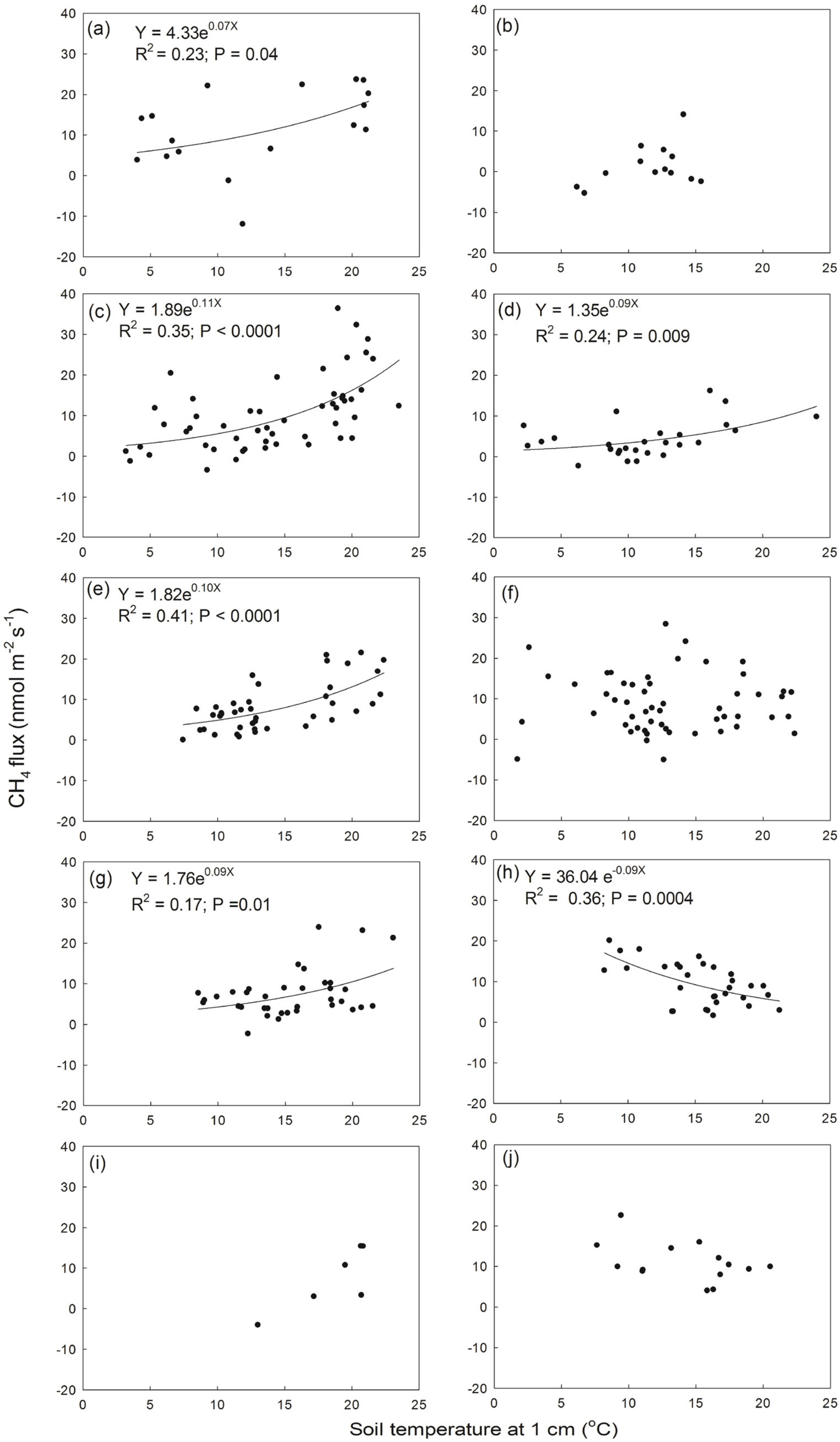

Fig. 7. The relationship between soil temperature at 1 cm and growing season CH_4 flux under different water table (WT) conditions. The left panel is for 2014 and the right one is for 2015. The panels from the top to the bottom were for WT range of -0.1 ~ -0.15 m (a, b), -0.15 ~ -0.2 m (c, d), -0.2 ~ -0.25 m (e, f), -0.25 ~ -0.30 m (g, h) and -0.30 ~ -0.35 m (i,j), respectively.

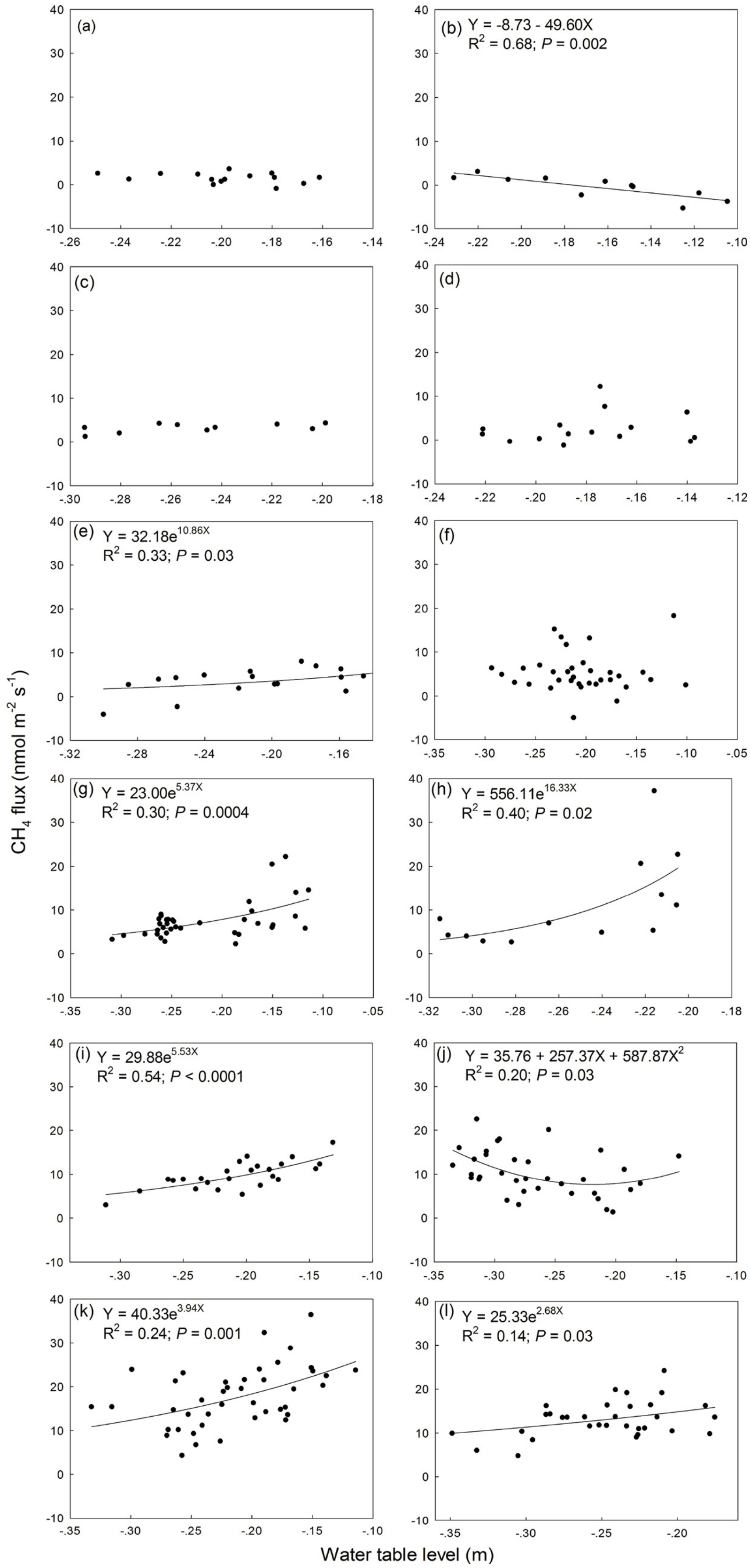

Fig. 8. The relationship between water table level and growing season CH_4 flux under different soil temperature conditions. The left panel is for 2014 and the right one for 2015. The panel from top to the bottom is for soil temperature at 50 cm of < 5 °C (a,b), 5–7 °C (c,d), 7–9 °C (e,f), 9–11 °C(g,h), 11–13 °C(i,j), > 13 °C(k,l).

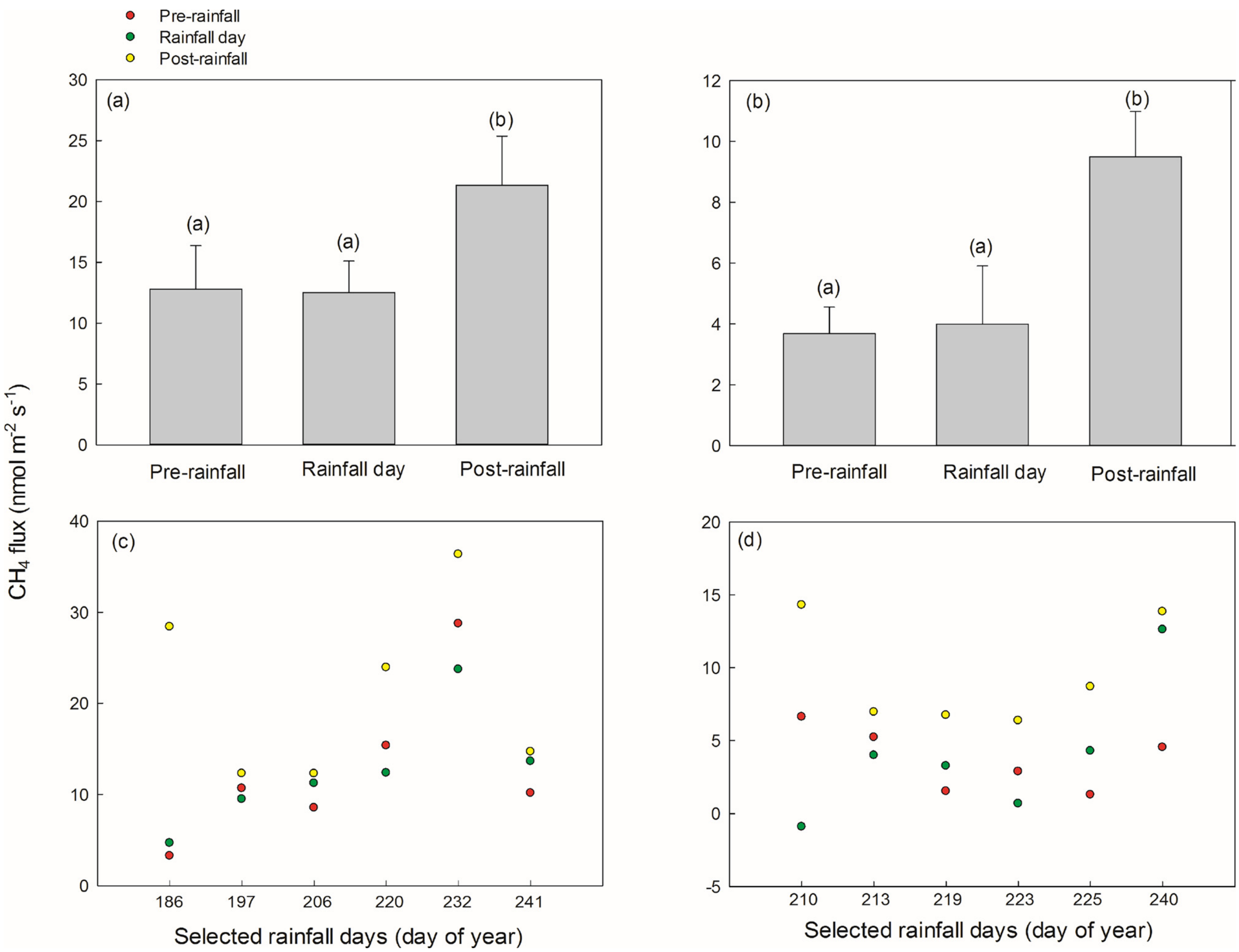

Fig. 9. The comparison of average CH_4 flux for all selected pre-rainfall, rainfall and post-rainfall days in 2014 (a) and 2015 (b).The paired comparison of CH_4 flux among one day before large rainfall, large rainfall day and one day after large rainfall day during the middle growing season in 2014 (c) and 2015 (d). Days with rainfall > 2 mm day^{-1} and the data availability of pre-rainfall, rainfall and post-rainfall days more than 70% were chosen.

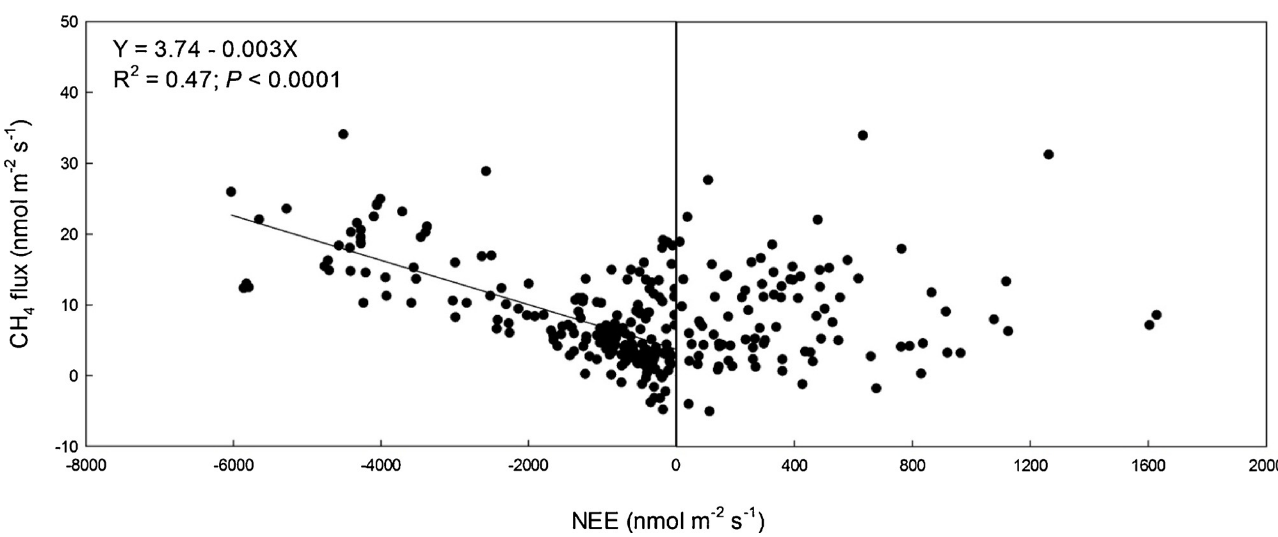

Fig. 10. Relationship between daily average net ecosystem exchange of CO_2 (NEE) and CH_4 flux during growing seasons of 2014 and 2015. Positive values of NEE indicate net emissions of CO_2 and negative values represent CO_2 sequestration from the atmosphere.

and pattern of precipitation might affect CH_4 flux. The underlying mechanism of how rainfall affects CH_4 flux are still unclear. In particular, this study highlights the importance of non-growing season CH_4 emissions in the estimation of annual CH_4 budget and uncertainty may exist in estimating non-growing season CH_4 emissions from empirical relationships only based on growing season data since the controls over CH_4 flux can be different between growing season and non-growing season.

Table 2
Cumulative CH_4 fluxes(g CH_4 m^{-2}) and estimated random uncertainty (RU, g CH_4 m^{-2}) and gap-filling uncertainties (GU, g CH_4 m^{-2}) for the different seasonal periods and their contributions to the annual emissions in two years, May 2014 to April 2015 and May 2015 to April 2016.

	2014-2015					2015-16				
Period	Duration days	CH_4 fluxes	RU	GU	Contribution %	Duration days	CH_4 fluxes	RU	GU	Contribution %
Growing season	178	2.2 ± 0.7	0.7	0.1	59	184	1.9 ± 0.8	0.6	0.6	61
Soil freezing	62	−0.1 ± 0.1	0.1	0.0	−2	45	0.0 ± 0.2	0.2	0.0	1
Winter	111	1.6 ± 0.5	0.1	0.5	43	122	1.1 ± 0.3	0.3	0.1	35
Soil thawing	14	−0.0 ± 0.1	0.1	0.0	0	15	0.1 ± 0.2	0.2	0.0	3
Total	365	3.7 ± 0.9	0.7	0.5		366	3.1 ± 0.9	0.7	0.8	

Growing season began and ended at the first seven consecutive days with daily air temperature above 5 ºC and below 5ºC, respectively; soil freezing, ranging from the end of the growing season to the first two consecutive days with average daily soil temperature below 0ºC at 5 cm depth; winter started at the end of the soil freezing period and ended when snow melted out (after seven consecutive days with average air temperature above 0 ºC); soil thawing period was between winter and the growing season.

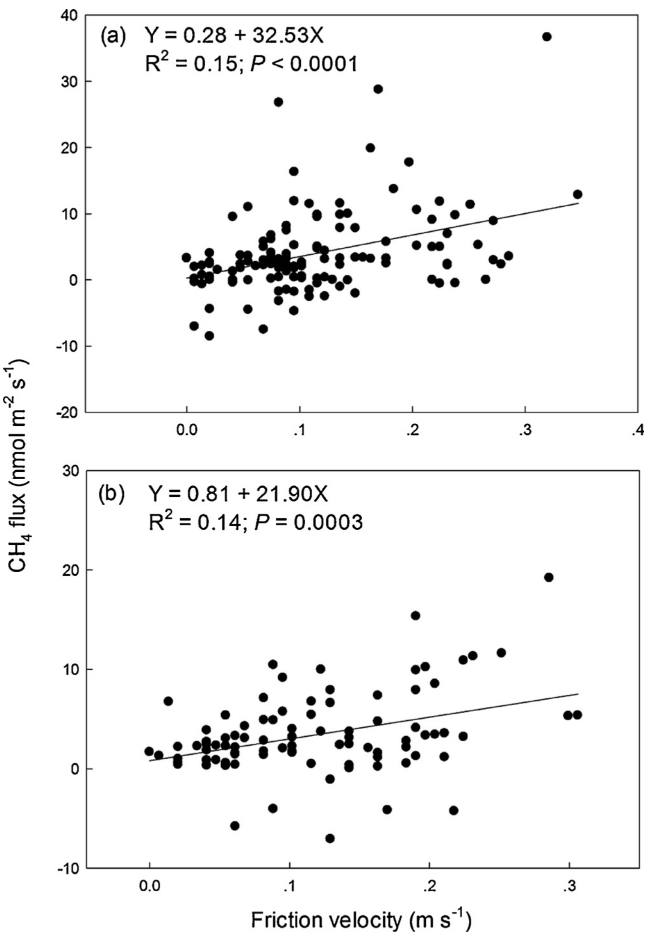

Fig. 11. Relationship between daily average CH_4 flux and friction velocity during the non-growing season in 2014 (a) and 2015(b).

Acknowledgments

This study was made possible by the support of the following funding to J. Wu: Natural Sciences and Engineering Research Council of Canada (NSERC)-Discovery Grant, Canada Foundation for Innovation-John R. Evans Leaders Fund, Research & Development Corporation (RDC, NL)- Leverage R&D, RDC-Ignite R&D, RDC-RCRI (Regional Collaborative Research Initiative), Agricultural Research Initiative (NL), Humber River Basin Research Initiative of NL, Grenfell Campus' Start-up Research Fund andVice-President Research Fund, and the Graduate Student Stipend funding from the Institute for Biodiversity, Ecosystem Science, and Sustainability (IBES, NL). M. Wang received a Graduate Student Baseline Fellowship from School of Graduate Studies, Memorial University and start-up research funding from South Normal University in China. Special thanks were given to Prof. Henry Mann for his help in vegetation identification, Ms. Denise Bouzane for her constructive guidance on the selection of our research site, the Department of Facility Management at Grenfell Campus, Memorial University for logistic support, and Mr. Keon Noseworthy for his help in the installation of our EC towers. Thanks for the constructive suggestions and comments from the two anonymous reviewers.

Appendix A. Supplementary data

Supplementary material related to this article can be found, in the online version, at doi:https://doi.org/10.1016/j.agrformet.2018.07.002.

References

Abdalla, M., Hasting, A., Truu, J., Espenberg, M., Mander, Ü., Smith, P., 2016. Emissions of methane from northern peatlands: a review of management impacts and implications for future management options. Ecol. Evol. 6, 7080–7102.
Alm, J., Talanov, A., Saarnio, S., Silvola, J., Ikonen, E., Aaltonen, H., Nykänen, H., 1997. Reconstruction of the carbon balance for microsites in a boreal oligotrophic pine fen, Finland. Oecologia 110 (3), 423–431.
Aubinet, M., Vesala, T., Papale, D., 2012. Eddy Covariance: a Practical Guide to Measurement and Data Analysis. Springer, Dordrecht, Heidelberg, London, New York.
Bellisario, L., Bubier, J., Moore, T., Chanton, J., 1999. Controls on CH_4 emissions from a northern peatland. Glob. Biogeochem. Cycles 13 (1), 81–91.
Bergamaschi, P., Frankenberg, C., Meirink, J.F., Krol, M., Dentener, F., Wagner, T., Platt, U., Kaplan, J.O., Körner, S., Heimann, M., Dlugokencky, E.J., Goede, A., 2007. Satellite chartography of atmospheric methane from SCIAMACHY on board ENVISAT: 2. Evaluation based on inverse model simulations. J. Geophys. Res.: Atmos. 112 (D2) 2006JD007268.
Bergamaschi, P., Frankenberg, C., Meirink, J.F., Krol, M., Krol, M., Villani, M.G., Houweling, S., Dentener, F., Dlugokencky, E.J., Miller, J.B., Gatti, L.V., Engel, A., Levin, I., 2009. Inverse modeling of global and regional CH_4 emissions using SCIAMACHY satellite retrievals. J. Geophys. Res. :Atmos. 114 (D22) 2009JD012287.
Bergman, I., Klarqvist, M., Nilsson, M., 2000. Seasonal variation in rates of methane production from peat of various botanical origins: effects of temperature and substrate quality. FEMS Microbiol. Ecol. 33 (3), 181–189.
Blodau, C., Basiliko, N., Moore, T.R., 2004. Carbon turnover in peatland mesocosms exposed to different water table levels. Biogeochemistry 67, 331–351.
Bridgham, S.D., Cadillo-Quiroz, H., Keller, J.K., Zhuang, Q., 2013. Methane emissions from wetlands: biogeochemical, microbial, and modeling perspectives from local to global scales. Global Change Biol. 19 (5), 1325–1346.
Brown, M.G., Humphreys, E.R., Moore, T.R., Roulet, N.T., Lafleur, P.M., 2014. Evidence for a nonmonotonic relationship between ecosystem-scale peatland methane emissions and water table depth. J. Geophys. Res.: Biogeosci. 119 (5) 2013JG002576.
Bubier, J., Moore, T., Roulet, N., 1993. Methane emissions from wetlands in the mid-boreal region of northern Ontario, Canada. Ecology 74 (8), 2240–2254.
Businger, J., 1986. Evaluation of the accuracy with which dry deposition can be measured with current micrometeorological techniques. J. Clim. Appl. Meteorol. 25 (8), 1100–1124.
Chen, H., Wu, N., Yao, S.P., Gao, Y.H., Wang, Y.F., Tian, J.Q., Yuan, X.Z., 2010. Diurnal variation of methane emissions from an alpine wetland on the eastern edge of Qinghai-Tibetan Plateau. Environ. Monit. Assess. 164 (1-4), 21–28.
Christensen, T.R., Ekberg, A., Ström, L., Mastepanov, M., Panikov, N., Öquist, M., Svensson, B.H., Nykänen, H., Martikainen, P.J., Oskarsson, H., 2003. Factors controlling large scale variations in methane emissions from wetlands. Geophys. Res.

Lett. 30 (7) 2002GL016848.
Dengel, S., Zona, D., Sachs, T., Aurela, M., Jammet, M., Parmentier, F.J.W., Oechel, W., Vesala, T., 2013. Testing the applicability of neural networks as a gap-filling method using CH_4 flux data from high latitude wetlands. Biogeosciences 10 (12), 8185–8200.
Dinsmore, K.J., Skiba, U.M., Billet, M.F., Rees, R.M., 2009. Effects of water table on greenhouse emissions from peatland mesocosms. Plant Soil 318, 229–242.
Elizondo, D.A., Góngora, M.A., 2005. Current trends on knowledge extraction and neural networks. In: Duch, W., Kacprzyk, J., Oja, E., Zadrozny, S. (Eds.), Artificial Neural Networks: Formal Models and Their Applications–ICANN 2005. Springer, Berlin, Heidelberg, pp. 752.
Finkelstein, P.L., Sims, P.F., 2001. Sampling error in eddy correlation flux measurements. J. Geophys. Rese.: Atmos. 106 (D4), 3503–3509.
Fortuniak, K., Pawlak, W., Bednorz, L., Grygoruk, M., Siedlecki, M., Zieliński, M., 2017. Methane and carbon dioxide fluxes of a temperate mire in Central Europe. Agric. For. Meteorol. 232, 306–318.
Frenzel, P., Karofeld, E., 2000. CH_4 emission from a hollow-ridge complex in a raised bog: the role of CH_4 production and oxidation. Biogeochemistry 51 (1), 91–112.
Frolking, S., Roulet, N.T., 2007. Holocene radiative forcing impact of northern peatland carbon accumulation and methane emissions. Global Change Biol. 13 (5), 1079–1088.
Frolking, S., Roulet, N., Fuglestvedt, J., 2006. How northern peatlands influence the earth's radiative budget: sustained methane emission versus sustained carbon sequestration. J. Geophys. Res.: Biogeosci. 111 (G1) 2005JG00009.
Goodrich, J.P., Campbell, D.I., Clearwater, M.J., Schipper, L.A., 2015. Overriding control of methane flux temporal varibility by water table dynamics in a Southern Hemisphere raised bog. J. Geophys. Res.: Biogeosci. 120, 819–831.
Granberg, G., Mikkelä, C., Sundh, I., Svensson, B.H., Nilsson, M., 1997. Sources of spatial variation in methane emission from mires in northern Sweden: a mechanistic approach in statistical modeling. Global Biogeochem. Cycles 11 (2), 135–150.
Günther, A.B., Huth, V., Jurasinski, G., Glatzel, S., 2014. Scale-dependent temporal variation in determining the methane balance of a temperate fen. Greenhouse Gas Meas. Manag. 4 (1), 41–48.
Hommeltenberg, J., Mauder, M., Drösler, M., Heidbach, K., Werle, P., Schimid, H.P., 2014. Ecosystem scale methane fluxes in a natural temperate bog-pine forest in southern Germany. Agric. For. Meteorol. 198, 273–284.
IPCC. Climate Change, 2014. In: Pachauri, R.K., Meyer, L.A. (Eds.), Synthesis Report. Contribution of Working Groups I, II and III to the Fifth Assessment Report of the Intergovernmental Panel on Climate Change. Geneva, Switzerland, pp. 1–151.
Jackowicz-Korczyński, M., Christensen, T.R., Bäckstrand, K., Crill, P., Friborg, T., Mastepanov, M., Ström, L., 2010. Annual cycle of methane emission from a subarctic peatland. J. Geophys. Res.: Biogeosci. 115 (G2) 2008JG000913.
Jain, A.K., Mao, J., Mohiuddin, K., 1996. Artificial neural networks: a tutorial. Computer (3), 31–44.
Järvi, L., Nordbo, A., Junninen, H., Riikonen, A., Moilanen, J., Nikinmaa, E., Vesala, T., 2012. Seasonal and annual variation of carbon dioxide surface fluxes in Helsinki, Finland, in 2006-2010. Atmos. Chem. Phys. 12 (18), 8475–8489.
Kane, E.S., Turetsky, M.R., Harden, J.W., McGuire, A.D., Waddington, J.M., 2010. Seasonal ice and hydrological controls on dissolved organic carbon and nitrogen concentrations in a boreal-rich fen. J. Geophys. Res. : Biogeosci. 115, G04012.
Kim, J., Verma, S.B., Billesbach, D.P., 1999. Seasonal variation in methane emission from a temperate phragmites-dominated marsh: effect of growth stage and plant-mediated transport. Global Change Biol. 5 (4), 433–440.
Kljun, N., Calanca, P., Rotach, M., Schmid, H., 2004. A simple parameterisation for flux footprint predictions. Boundary Layer Meteorol. 112 (3), 503–523.
Koebsch, F., Glatzel, S., Jurasinski, G., 2013. Vegetation controls methane emissions in a coastal brackish fen. Wetlands Ecol. Manage. 21 (5), 323–337.
Koebsch, F., Jurasinski, G., Koch, M., Hofmann, J., Glatzel, S., 2015. Controls for multi-scale temporal variation in ecosystem methane exchange during the growing season of a permanently inundated fen. Agric. For. Meteorol. 204, 94–105.
Kowalska, N., Chojnicki, B.H., Rinne, J., Haapanala, S., Siedlecki, P., Urbaniak, M., Juszczak, R., Olejnik, J., 2013. Measurements of methane emission from a temperate wetland by the eddy covariance method. Int. Agrophys. 27 (3), 283–290.
Lai, D.Y., Roulet, N.T., Moore, T.R., 2014. The spatial and temporal relationships between CO_2 and CH_4 exchange in a temperate ombrotrophic bog. Atmos. Environ. 89, 249–259.
Liblik, L., Moore, T., Bubier, J., Robinson, S., 1997. Methane emissions from wetlands in the zone of discontinuous permafrost: Fort Simpson, Northwest Territories, Canada. Global Biogeochem. Cycles 11 (4), 485–494.
Liu, D., Ding, W., Yuan, J., Xiang, J., Lin, Y., 2014. Substrate and/or substrate-driven changes in the abundance of methanogenic archaea cause seasonal variation of methane production potential in species-specific freshwater wetlands. Appl. Microbiol. Biotechnol. 98 (10), 4711–4721.
Long, K.D., Flanagan, L.B., Cai, T., 2010. Diurnal and seasonal variation in methane emissions in a northern Canadian peatland measured by eddy covariance. Global Change Biol. 16 (9), 2420–2435.
Luan, J., Wu, J., 2014. Gross photosynthesis explains the 'artificial bias' of methane fluxes by static chamber (opaque versus transparent) at the hummocks in a boreal peatland. Environ. Res. Lett. 9 (10), 105005.
Luan, J., Wu, J., 2015. Long-term agricultural drainage stimulates CH_4 emissions from ditches through increased substrate availability in a boreal peatland. Agric. Ecosyst. Environ. 214, 68–77.
MacDonald, J., Fowler, D., Hargreaves, K.J., Skiba, U., Leith, I.D., Murray, M.B., 1998. Methane emission rates from a northern wetland; response to temperature, water table and transport. Atmos. Environ. 32 (19), 3219–3227.
Mauder, M., Foken, T., 2011. Documentation and instruction manual of the eddy-covariance software package TK3. Universität Bayreuth. Abteilung Mikrometeorologie: Arbeitsergebnisse 46, 60 ISSN 1614-8924.
Metje, M., Frenzel, P., 2007. Methanogenesis and methanogenic pathways in a peat from subarctic permafrost. Environ. Microbiol. 9 (4), 954–964.
Mikaloff Fletcher, S.E., Tans, P.P., Bruhwiler, L.M., Miller, J.B., Heimann, M., 2004. CH4 sources estimated from atmospheric observations of CH4 and its $^{13}C/^{12}C$ isotopic ratios: inverse modeling of source processes. Global Biogeochem. Cycles 18 (4) 2004GB002223.
Mikkelä, C., Sundh, I., Svensson, B.H., Nilsson, M., 1995. Diurnal variation in methane emission in relation to the water table, soil temperature, climate and vegetation cover in a Swedish acid mire. Biogeochemistry 28 (2), 93–114.
Moffat, A.M., Papale, D., Reichstein, M., Hollinger, D.Y., Richardson, A.D., et al., 2007. Comprehensive comparison of gap-filling techniques for eddy covariance net carbon fluxes. Agric. For. Meteorol. 147 (3), 209–232.
Moffat, A.M., Beckstein, C., Churkina, G., Mund, M., Heimann, M., 2010. Characterization of ecosystem responses to climatic controls using artificial neural networks. Global Change Biol. 16 (10), 2737–2749.
Moncrieff, J.B., Massheder, J.M., Bruin, H.D., Elbers, J., Frobprg, T., Heusinkveld, B., Kabat, P., Scott, S., Soegaard, H., Verhoef, A., 1997. A system to measure surface fluxes of momentum, sensible heat, water vapour and carbon dioxide. J. Hydrol. 188, 589–611.
Moncrieff, J., Clement, R., Finnigan, J., Meyers, T., 2004. Averaging, detrending, and filtering of eddy covariance time series, handbook of micrometeorology. A Guide for Surface Flux Measurement and Analysis. Kluwer Academic Publishers, Dordrecht, pp. 7–31.
Moore, T., Knowles, R., 1989. The influence of water table levels on methane and carbon dioxide emissions from peatland soils. Can. J. Soil Sci. 69 (1), 33–38.
Nguyen, H.H., Chan, C.W., 2004. Multiple neural networks for a long term time series forecast. Neural Comput. Appl. 13 (1), 90–98.
Nijp, J.J., Limpens, J., Metselaar, K., Peichl, M., Nilsson, M.B., Zee, S.E.A.T.M., Berendse, F., 2015. Rain events decrease boreal peatland net CO_2 uptake through reduced light availability. Global Change Biol. 21, 2309–2320.
Nilsson, M., Mikkelä, C., Sundh, Granberg, G., Svensson, B.H., Ranneby, B., 2001. Methane emission from Swedish mires: national and regional budgets and dependence on mire vegetation. J. Geophys. Res.: Atmos. 106 (18), 20847–20860.
Nilsson, M., Sagerfors, J., Buffam, I., Laudon, H., Eriksson, T., Grelle, A., Klementsson, L., Weslien, P., Lindroth, A., 2008. Contemporary carbon accumulation in a boreal oligotrophic minerogenic mire-a significant sink after accounting for all c-fluxes. Global Change Biol. 14 (10), 2317–2332.
Olson, D., Griffis, T., Noormets, A., Kolka, R., Chen, J., 2013. Interannual, seasonal, and retrospective analysis of the methane and carbon dioxide budgets of a temperate peatland. J. Geophys. Res.: Biogeosci. 118 (1), 226–238.
Papale, D., Reichstein, M., Aubinet, M., Canfora, E., Bernhofer, C., Kutsch, W., Longdoz, B., Rambal, S., Valentini, R., Vesala, T., Yakir, D., 2006. Towards a standardized processing of net ecosystem exchange measured with eddy covariance technique: algorithms and uncertainty estimation. Biogeosciences 3 (4), 571–583.
Petrescu, A., van Beek, L.P.H., van Huissteden, J., Prigent, C., Sachs, T., Corradi, C.A.R., Parmentier, F.J.W., Dolman, A.J., 2010. Modeling regional to global CH4 emissions of boreal and arctic wetlands. Global Biogeochem. Cycles 24 (4) 2009GB003610.
Prather, M., Ehalt, D., Dentener, F., Derwent, R., Dlugokencky, E., Holland, E., Isaksen, I., Katima, J., Kirchho, V., Matson, P., Midgley, P., Wang, M., 2001. Atmospheric chemistry and greenhouse gases. In: Houghton, J.T., Ding, Y., Griggs, D.J., Noguer, M., van der Linden, P.J., Dai, X., Maskell, K., Johnson, C.A. (Eds.), Climate Change: the Scientific Basis-Contribution of Working Group 1 to the Third Assessment Report of the Intergovenmental Panel on Climate Change. Cambridge Univerisity Press, Cambridge, New York.
Pypker, T., Moore, P., Waddington, J., Hribljan, J., Chimner, R., 2013. Shifting environmental controls on CH_4 fluxes in a sub-boreal peatland. Biogeosciences 10 (12), 7971–7981.
Riedmiller, M., 1994. Rprop-Description and Implementation Details, Technical Report. Inst. für Logik, Komplexität und Deduktionssysteme Univ., Karlsruhe, Germany.
Roulet, N.T., 2000. Peatlands, carbon storage, greenhouse gases, and the Kyoto protocol: prospects and significance for Canada. Wetlands 20 (4), 605–615.
Sachs, T., Wille, C., Boike, J., Kutzbach, L., 2008. Environmental controls on ecosystem-scale CH_4 emission from polygonal tundra in the Lena River Delta, Siberia. J. Geophys. Res.: Biogeosci. 113 (G3) 2007JG000505.
Skov, K., 2014. Spatiotemporal variability in methane emission from an Arctic fen over a growing season: dynamics and driving factors. Student Thesis INES. Department of Physical Geography and Ecosystem Science, Lund Univeristy.
Song, W., Wang, H., Wang, G.S., Chen, L.T., Jin, Z.N., Zhuang, Q.L., He, J.S., 2015. Methane emissions from an alpine wetland on the Tibetan Plateau: neglected but vital contribution of the nongrowing season. J. Geophys. Res.: Biogeosci. 120 (8), 1475–1490.
Svensson, B.H., 1984. Different temperature optima for methane formation when enrichments from acid peat are supplemented with acetate or hydrogen. Appl. Environ. Microbiol. 48 (2), 389–394.
Treat, C.C., Bubier, J.L., Varner, R.K., Crill, P.M., 2007. Timescale dependence of environmental and plant-mediated controls on CH_4 flux in a temperate fen. J. Geophys. Res.: Biogeosci. 112 (G1), G01014.
Turetsky, M., Treat, C.C., Waldrop, M.P., Waddington, J.M., Harden, J.W., McGuire, A.D., 2008. Short-term response of methane fluxes and methanogen activity to water table and soil warming manipulations in an Alaskan peatland. J. Geophys. Research: Biogeosci. 113 (G3) 2007JG000496.
Turetsky, M.R., Kotowska, A., Bubier, J., Dise, N.B., Crill, P., et al., 2014. A synthesis of methane emissions from 71 northern, temperate, and subtropical wetlands. Global Change Biol. 20 (7), 2183–2197.
Vanselow-Algan, M., Schmidt, S.R., Greven, M., Fiencke, C., Kutzbach, L., Pfeiffer, E.M.,

2015. High methane emissions dominated annual greenhouse gas balances 30 years after bog rewetting. Biogeosciences 12 (14), 4361–4371.
Vickers, D., Mahrt, L., 1997. Quality control and flux sampling problems for tower and aircraft data. J. Atmos. Oceanic Technol. 14 (3), 512–526.
Waddington, J., Roulet, N., 1996. Atmosphere-wetland carbon exchanges: scale dependency of CO2 and CH_4 exchange on the developmental topography of a peatland. Global Biogeochem. Cycles 10 (2), 233–245.
Wang, M., Wu, J., Lafleur, P.M., Luan, J., Chen, H., Zhu, X., 2018. Can abandoned peatland pasture sequestrate more carbon dioxide from the atmosphere than an adjacent pristine bog in Newfoundland, Canada? Agric. For. Meteorol. 248, 91–108.
Webb, E.K., Pearman, G.I., Leuning, R., 1980. Correction of flux measurements for density effects due to heat and water vapour transfer. Q. J. R. Meteorolog. Soc. 106 (447), 85–100.
Whiting, G., Chanton, J., 1993. Primary production control of methane emission from wetlands. Nature 364, 794–795.
Wilczak, J.M., Oncley, S.P., Stage, S.A., 2001. Sonic anemometer tilt correction algorithms. Boundary Layer Meteorol. 99 (1), 127–150.
Wille, C., Kutzbach, L., Sachs, T., Wagner, D., Pfeiffer, E., 2008. Methane emission from Siberian arctic polygonal tundra: eddy covariance measurements and modeling. Global Change Biol. 14 (6), 1395–1408.
Williams, R.T., Crawford, R.L., 1984. Methane production in Minnesota peatlands. Appl. Environ. Microbiol. 47 (6), 1266–1271.
Zhuang, Q., Melillo, J.M., Kicklighter, D.W., Prinn, R.G., McGuire, A.D., Steudler, P.A., Felzer, B.S., Hu, S., 2004. Methane fluxes between terrestrial ecosystems and the atmosphere at northern high latitudes during the past century: a retrospective analysis with a process-based biogeochemistry model. Global Biogeochem. Cycles 18 (3).
Zhuang, Q., Melillo, J.M., Sarofim, M.C., et al., 2006. CO_2 and CH_4 exchanges between land ecosystems and the atmosphere in northern high latitudes over the 21st century. Geophys. Res. Lett. 33 (17) 2006GL026972.